Astron. Astrophys. 325, 563–568 (1997)

ASTRONOMY
AND
ASTROPHYSICS

The δ Scuti star θ Tucanae*

II. $uvby$ colour variations and pulsational/orbital properties

C. Sterken[1,**]

University of Brussels (VUB), Pleinlaan 2, B-1050 Brussels, Belgium

Received 5 February 1997 / Accepted 24 March 1997

Abstract. On the basis of almost 1500 $uvby$ photometric observations of θ Tucanae collected in 1993, we discuss the colour variation of this multi-periodic δ Scuti star and debate some of its binary and pulsational properties. The frequencies f_1 = 0.281 and f_2 = 0.142 cd^{-1} embody orbital motion in a 7$^{\rm d}$.04 day ellipsoidal configuration characterised by a light curve with unequal maxima and minima and a colour index that becomes bluer during the minimum phases. The first results of an analysis of the light curve points towards a mass ratio q of the order of 0.10–0.15. We present dependable numerical values for colour phase differences and amplitude ratios $A_{\rm b-y}/A_{\rm y}, \phi_{\rm b-y} - \phi_{\rm y}, A_{\rm v-y}/A_{\rm y}, \phi_{\rm v-y} - \phi_{\rm y}$ and $A_{\rm u-y}/A_{\rm y}, \phi_{\rm u-y} - \phi_{\rm y}$ which can be used for pulsation-mode identification. The principal pulsation frequency f_7 = 20.28 cd^{-1} is reconcilable with a radial mode.

Key words: stars: individual: θ Tuc – stars: oscillations – stars: δ Scuti stars – stars: binaries: general

1. Introduction

θ Tuc (HR 139, V = 6.11, A4) is a multi-periodic δ Scuti star with V-amplitude $\sim 0^{\rm m}.08$ and principal period $\sim 1^{\rm h}11^{\rm m}$. Prompted by a suggestion by Kurtz ("A proposal for new observations of θ Tuc", Kurtz 1988), we organised a multi-site observing campaign incorporating 2300 new Strömgren y and Johnson V photometric observations collected during 246 hours at three sites (Paparó et al. 1996, henceforth referred to as Paper I). From a Fourier analysis of these data an adequate description of the V light variation in terms of 13 frequencies was worked out. Ten frequencies were found in the range of 15.8 to 20.28 cycles per day (cd^{-1}); they are distributed in groups and these groups are equally spaced. These frequencies are constant in amplitude on a short time scale. Two frequencies, 0.282 and 0.142 cd^{-1}(3.56 and 7.04 days period) were found to represent the variation of the night-to-night mean light level of θ Tuc, and led to the suggestion that the δ Scuti star is the primary in a binary system with a late F type companion.

In the present paper we describe the Strömgren $uvby$ data collected in the same campaign, and discuss some of the pulsational properties of the δ Scuti star.

Table 1. Overview of available $uvby$ data and mean errors in each band. Δ is the magnitude difference between comparison stars, σ is the associated mean error in millimag, R the average time resolution of the variable-star data (in minutes)

Δ_y	σ_y	Δ_b	σ_b	Δ_v	σ_v	Δ_u	σ_u	R
-1.358	4	-1.430	4	-1.584	4	-1.743	5	5

2. The new data

We refer to Paper I for details on the instrumentation and for the journal of observations. We remind that all our magnitudes are differential, using C_1 = HR 83 (π Tuc, V = 5.49, B9V) and C_2 = HR 169 (V = 6.86, A0) as comparison stars. Our new data are u, v, b magnitudes collected simultaneously with the y magnitudes using the SAT $uvby$ photometer in Chile. Table 1 gives the mean magnitude differences between comparison stars with the subsequently derived mean error on one single differential measurement, and the approximate time resolution (in minutes) of the measurements of θ Tuc (the mean error is derived from consecutive $C_1 - C_2$ data, differential θ Tuc magnitudes have been obtained by subtracting $(C_1 + C_2)/2$ from the corresponding measured magnitude of the variable star).

Figs. 1 and 2 illustrate sample Strömgren light and colour curves, for comparison with the other data we refer to Fig. 5 of Paper I. The continuous curves represent the calculated 13–frequency light- and colour curves for $y, b, v, u, b-y, v-b$ and $u-v$. Note the strong increase of amplitude from y to u.

* Based on observations obtained at the European Southern Observatory, La Silla, Chile (Program 51-7-038)

** Belgian Fund for Scientific Research (FWO)

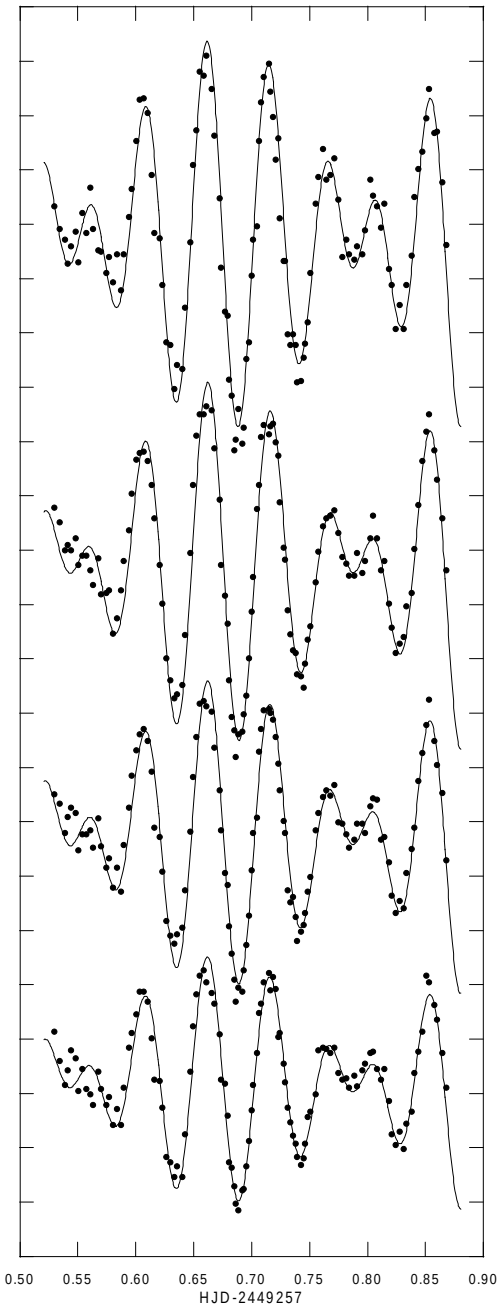

Fig. 1. Selected y, b, v, u (bottom to top) light curves of θ Tuc . Tick marks on y-axis are $0\overset{\text{m}}{.}01$ apart

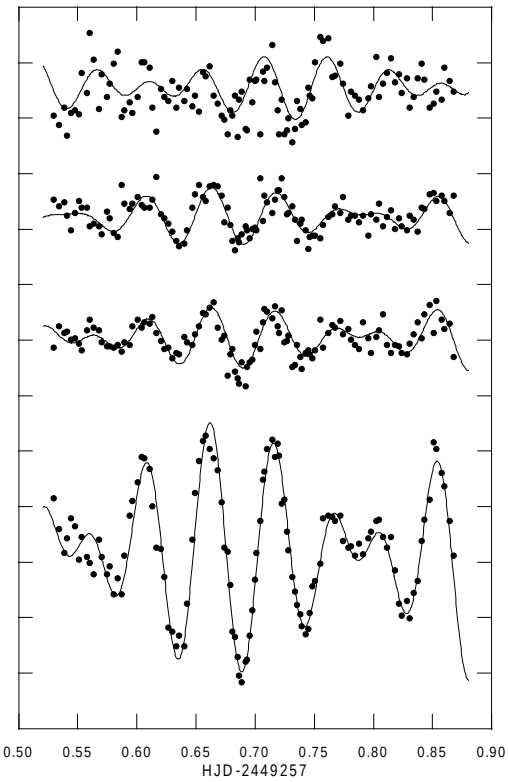

Fig. 2. Selected $y, b-y, v-b, u-v$ (bottom to top) light curves of θ Tuc

3. Colour dependence of amplitudes and phases

The data set contains 1450 $uvby$ measurements spread over 42 observing days. We have fitted the 13 frequencies of Paper I to these data, and the results are given in Table 2, see also Fig. 1. The fit yields consistent solutions in amplitude and phase for each band, with resulting residuals of, respectively, $0\overset{\text{m}}{.}0039$, $0\overset{\text{m}}{.}0041$, $0\overset{\text{m}}{.}0047$ and $0\overset{\text{m}}{.}0055$, quite comparable to the photometric accuracy given in Table 1. Table 2 also gives the average phase angle (in degrees, defined by $m(t) = m_o + \sum_{i=1}^{13} A_i cos[2\pi(t-t_o) - \varphi_i]$, m_0 being the mean light level in the appropriate band, and t_0 = 244 9249.0), and the amplitude ratios $A_{\rm b-y}/A_y, A_{\rm v-y}/A_y, A_{\rm u-y}/A_y$ and phase difference $\phi_{\rm b-y} - \phi_{\rm y}, \phi_{\rm v-y} - \phi_{\rm y}, \phi_{\rm u-y} - \phi_{\rm y}$ (see Sect. 5). In addition, the standard deviation σ_ϕ derived from averaging $\phi_u, \phi_v, \phi_b, \phi_y$ is given for the purpose of illustrating wavelength dependence (see further). The mean error on a single phase is given in Paper I and does not exceed 4.6° for f_3–f_{12} and equals 0.8°, 1.9° and 4.8°, respectively for f_1, f_2 and f_{13}.

Fig. 3 shows the amplitudes of the 13-frequency fit for each photometric band. Frequencies are arranged, from left to right in each block, in increasing order, the error bar represents the average mean error (σ) over all frequencies as derived in Paper I. It is immediately evident that the displayed pattern shows a high degree of internal consistency, at least for the 10 "pulsational" frequencies. There is a common trend that the amplitudes of the frequencies f_3–f_{12} increase towards shorter wavelengths. The amplitudes associated with the lowest frequencies (f_1, f_2) are smallest in b and appear of alternating strength from one colour band to the other. Though part of this could be explained as being within the expected error, this is certainly not so for the y band and out of question for the even smaller amplitudes associated with f_3–f_{12}. The amplitudes associated with f_{13} = 0.9935 are about equal in all bands.

Fig. 4 displays the behaviour of the phases: a similar internal consistency is seen for f_3–f_{12}. The lower frequencies have rather similar phases in each band, except perhaps for the $\phi_u(f_1)$ and

Table 2. 13–frequency fit to all $uvby$ data. A and ϕ are the amplitudes (in millimag) and phases (in degrees) in each band, and σ_ϕ is the calculated standard deviation over the four bands for each frequency. A_i, ϕ_i stand for $(A_{\rm b-y}/A_y, \phi_{\rm b-y} - \phi_{\rm y}), (A_{\rm v-y}/A_y, \phi_{\rm v-y} - \phi_{\rm y})$ and $(A_{\rm u-y}/A_y, \phi_{\rm u-y} - \phi_{\rm y})$

f	cd^{-1}	A_y	A_b	A_v	A_u	ϕ_y	ϕ_b	ϕ_v	ϕ_u	σ_ϕ	A_1	ϕ_1	A_2	ϕ_2	A_3	ϕ_3
1	0.2815	9.6	7.0	4.2	4.4	178.2	177.6	179.8	171.5	3.6						
2	0.1421	3.8	2.5	2.0	5.5	265.9	264.1	253.8	265.4	5.7						
3	17.0629	6.3	7.6	9.1	8.5	81.8	82.0	86.3	76.9	3.8	.225	3.8	.482	13.4	.352	-17.3
4	18.0630	4.0	5.0	5.9	6.3	51.7	47.9	49.6	35.1	7.5	.223	-14.5	.450	-1.0	.641	-43.8
5	19.0204	4.5	5.6	6.6	7.1	344.4	342.4	345.7	335.9	4.4	.280	-12.0	.484	3.5	.661	-23.7
6	15.8625	4.0	5.1	6.1	6.0	341.6	341.1	343.2	332.9	4.6	.286	0.8	.543	7.3	.545	-22.7
7	20.2806	15.0	18.4	20.8	24.3	82.5	82.7	83.7	77.8	2.7	.226	-0.2	.386	3.6	.626	-12.3
8	19.7941	3.8	4.7	5.3	5.4	124.3	123.6	125.1	117.0	3.7	.247	-2.5	.410	2.8	.476	-23.1
9	15.9462	4.0	5.1	6.1	5.6	184.3	182.2	184.0	176.5	3.6	.247	-9.9	.506	-2.2	.388	-28.2
10	20.1114	5.6	6.8	7.7	8.3	173.8	176.1	178.9	172.8	2.7	.239	9.4	.405	15.5	.491	-3.2
11	17.5418	1.4	1.9	2.2	2.3	300.5	294.8	303.1	297.9	3.6	.392	-14.8	.622	10.5	.713	-3.7
12	17.8566	1.3	1.8	1.9	1.9	240.3	233.5	239.7	220.0	9.4	.397	-21.2	.458	0.6	.641	-47.6
13	0.9935	1.8	1.5	2.0	2.3	48.0	46.8	48.3	35.5	6.1						

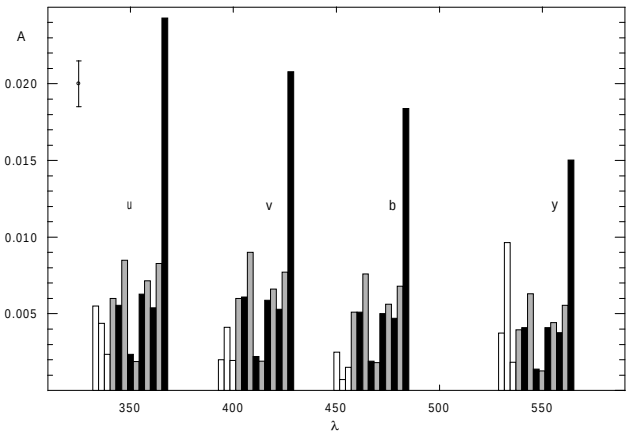

Fig. 3. $uvby$ amplitudes for each detected frequency (ordered by increasing frequency in each block, hatched and dark areas stand for f_3–f_{12})

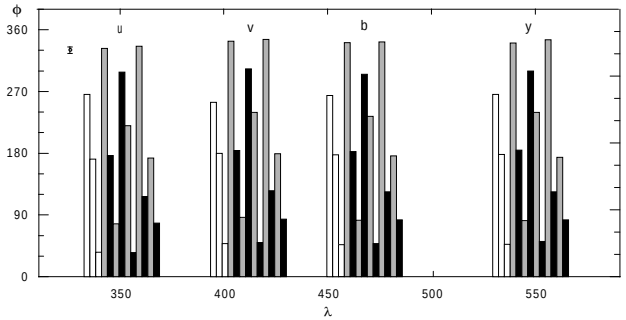

Fig. 4. $uvby$ phases (in $^\circ$) for each detected frequency (ordered by increasing frequency in each block). The error bar covers 2σ and is valid for f_1 and f_3–f_{12}, see text

$\phi_v(f_2)$ which show a substantial deviation that could indicate that the orbital light curve changes with time.

4. Colour changes through the orbital cycle

We have prewhitened the u, v, b, y and $b - y$ data with the 10 frequencies f_3–f_{12}, and present the result in bins of 0.005 orbital phase (P = 7$^{\rm d}$.04) in Fig. 5. Phase zero has been identified with the time of the deepest minimum which, for the sake of this discussion, we label "primary minimum" (the other minumum we call the secondary minimum, with corresponding nomenclature for the maxima). The orbital y light curve shows a succession of alternating minima of unequal depth; this is also so for the b, v and u bands, but the secondary minimum becomes progressively shallower towards shorter wavelengths. In addition, the maxima are of different height. The primary minima seem to be broader than the secondary minima, and there is even an indication that the bottom is neither flat nor well-rounded, thus revealing a slight discontinuity feature which, unfortunately, is not very densely covered by the data. As expected, the observational scatter increases towards u, see also Fig. 2. The $b - y$ colour index is anti-correlated with magnitude bahaviour in the four bands: the system is bluer during the minimum phases.

The form of the light curve is typical for an ellipsoidal variable, a non-eclipsing binary in which one or both stars is elongated by mutual gravitational forces. Radiative interaction (reflection effect) and strong limb-darkening effects on the pointed end of the elongated star can contribute to unequal minima (for an introduction, see Hall 1996). It is not clear whether the disturbed minimum features represent (grazing) eclipses or whether they possibly are the evidence of an accretion disk. The light curves in Fig. 5 show a striking similarity as the ones displayed in Fig. 2 of Mantegazza & Poretti (1995) for the ellipsoidal variable HD 96008 (including the fact that the system is bluer during the minimum phases).

Fig. 6 gives the amplitude of both minima and maxima in function of wavelength. It is evident that these amplitudes decrease from y towards v, with stationary values in the u band—note that the secondary minimum and maximum are rather poorly defined in the u band, though the primary minimum in that band is rather deep. Using formula (4) from Morris (1985),

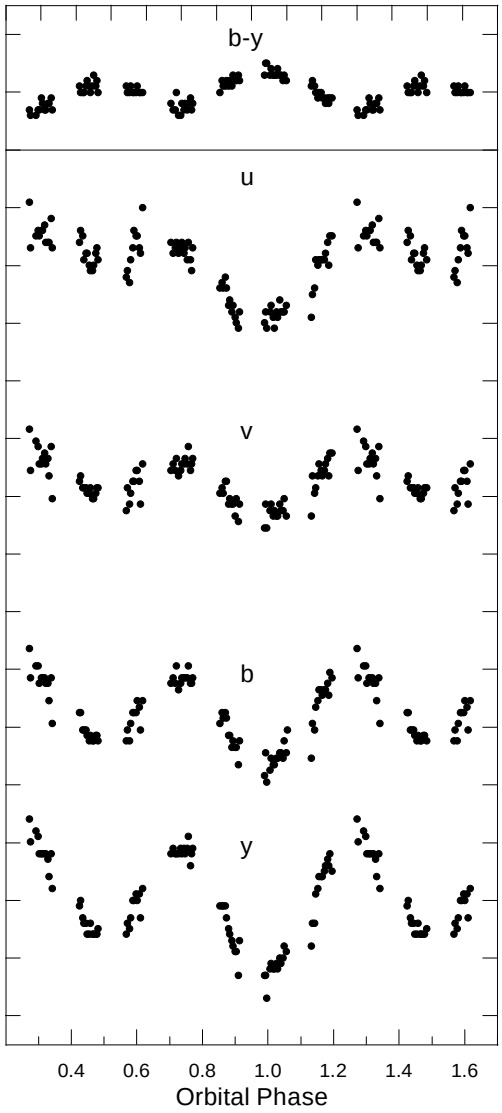

Fig. 5. $uvby$ and $b-y$ in function of orbital phase (P = 7.d04) after removal of all non-orbital frequencies. Data have been binned in intervals of 0.005 ($\sim$ 50 min), only bins with at least five data points were retained. Tick marks on the Y-axis are 0.m01 apart. Zero phase was chosen to coincide with the time of deepest minimum.

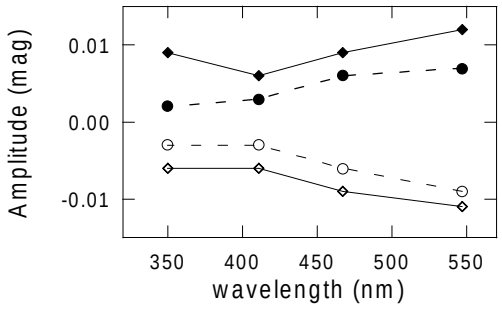

Fig. 6. Amplitudes of extrema of the orbital light curve in function of wavelength. Top to bottom: primary (———) and secondary minimum (– – –), respectively, secondary (– – –) and primary maximum (———)

and assuming that the bulk of the light variation is due to ellipsoidality, we obtain for the peak-to-peak amplitude of the primary star alone, 0.m046 in y, 0.m036 in b, 0.m024 in v and 0.m030 in u. The average difference between primary and secondary maximum is 0.m0027 $\pm$ 0.m0003. With the gravity-darkening coefficient τ = 0.3 (formula 4 from Morris 1985 using β = 0.08 and $T_{\rm eff}$ = 8000) and the limb-darkening coefficients u_1 from the tables of Al-Naimiy (1978)—using $v \sin i$ = 80 as in Paper I—the solution of Morris' equations (6)–(9) yields an estimate for the mass ratio q of 0.15 for the y and 0.10 for the b orbital light curve data. The values for u and v are of the order of 0.05, though cannot be trusted due to the peculiar form of the orbital light curves at shorter wavelengths. It is obvious that we are dealing with a peculiar (binary) configuration, and that a complete solution of the system must wait for a full spectrographic coverage. Again, we draw the attention to the similarities between the orbital light curves of the HD 96008 and the θ Tuc system.

5. Pulsation modes: the observables

By comparing the empirically-derived pulsation constant $Q = P\rho^{1/2}$ (where ρ equals the mean density) with theoretically-derived Q values, it should in principle be possible to derive the degree and order of the pulsation modes. In Paper I a range $0.018 < Q < 0.024$ (s.d. = 0.0019) for the pulsational frequencies f_3–f_{12} was derived, a value close to expected radial fundamental or first overtone values. Note that the small error on Q only reflects the very limited range of frequencies, and that the absolute error on the resulting Q value is much larger when the uncertainties on the values of luminosity and effective temperature are considered (the uncertainty on $T_{\rm eff}$ alone could easily increase Q by 0.05 d).

Multicolour photometry contains information about l because the light amplitudes and phases in different bands depend on the temperature and gravity variations. Watson (1988) expressed the light variation due to a single pulsation mode as a trigonometric function of the pulsation frequency and the phase shift between the variation of the local effective temperature $\mathscr{B}$ and the local fractional radius amplitude Ψ, and he derived diagrams of relative colour-to-visual amplitude versus visual phase differences (actually, $A_{\rm B-V}/A_{\rm V}$ and $\phi_{\rm B-V} - \phi_{\rm V}$) as a function of l. Apart from l, the points in that diagram, naturally, depend on the equilibrium parameters of the star. Garrido et al. (1990) presented such diagrams in the $uvby$ system for δ Scuti stars, and showed that diagrams based on $b-y$ or $v-y$ can discriminate between radial and low-order non-radial pulsations. Combinations including the u filter, though, do not allow such segregation, but are more useful for calculating phase angles for temperature and gravity variations. Fig. 7 illustrates the range of $A_{\rm u-y}/A_{\rm y}$, $A_{\rm v-y}/A_{\rm y}$ and $A_{\rm b-y}/A_{\rm y}$ versus $\phi_{\rm u-y} - \phi_{\rm y}$, $\phi_{\rm v-y} - \phi_{\rm y}$ and $\phi_{\rm b-y} - \phi_{\rm y}$. Such amplitude ratios are only useful when significant, therefore some low-amplitude data (especially in b and v) will not be applicable. The spread in colour/amplitude

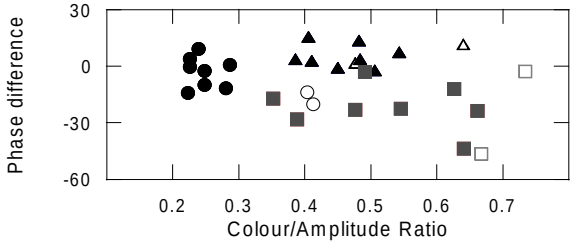

Fig. 7. Colour/amplitude ratio versus phase difference for all pulsational frequencies: $\circ : b-y$, $\triangle : v-y$, $\square : u-y$. Filled symbols correspond to frequencies that have visual amplitudes exceeding 2 mmag, viz. f_3–f_{10}

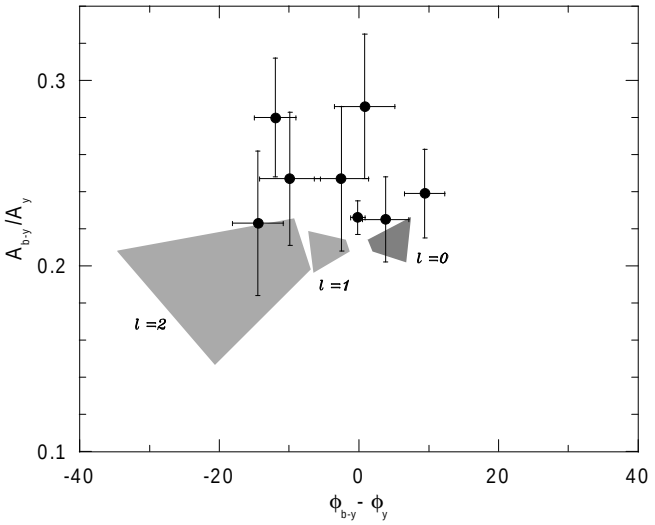

Fig. 8. Colour/amplitude ratio versus phase difference [$A_{\rm b-y}/A_{\rm y}$, $\phi_{\rm b-y} - \phi_{\rm y}$] diagram adopted from Fig. 4 of Garrido et al. (1990). The hatched areas indicate the loci of interest for $l = 0, 1, 2$ for all frequencies with visual amplitudes exceeding $0\overset{\rm m}{.}002$ (f_3–f_{10}). The error bars indicate the estimated maximum error derived from the mean errors on the amplitudes and phases

ratios noticeably increases when invoking the v and u bands. The points corresponding to f_{11} and f_{12}, the frequencies with y-amplitudes below 2 mmag, fall outside the locus corresponding to the other frequencies. Excluding those frequencies, we obtain average $A_{\rm b-y}/A_{\rm y}$ and $\phi_{\rm b-y} - \phi_{\rm y}$ with standard deviations, respectively, of 0.026 and 8.4°. We stress here that we do not imply that averaging over these frequencies has a physical meaning: the standard deviation simply shows that the spread of these independent quantities indicates that the mean errors, as shown in Fig. 8, are somewhat pessimistic (though our errors are quite comparable to those shown by Garrido et al. 1990 and by Watson 1988). This, however, is not the case for the $v-y$ and $b-y$ ratios where the amplitude ratios have a two-to-five times larger spread.

Fig. 8 is based on Fig. 4 of Garrido et al. (1990) and gives the areas of interest (regions corresponding to a particular l valid for δ Scuti stars) for $l = 0, 1, 2$ modes for a $T_{\rm eff}$ = 7850 K, $\log g = 4.0, Q = 0.03$ δ Scuti star model (a configuration very close to the standard model (8000, 4.0, 0.03) as selected by Watson (1988) for convenient use of model-atmosphere data. Only points corresponding to amplitudes that (within the errors) amount to 4 mmag are shown. Error bars correspond to the maximal error as calculated from the m.e. on the related quantities.

The diagram vividly shows that the situation is not clear-cut and that only some $l = 0, 1$ or 2 modes should be possible for θ Tuc—that is, assuming that θ Tuc can be represented by a stellar model as the one used by Garrido et al. (1990). Considering the fact that the corresponding quantities for the principal frequency might well be more accurate than suggested by the error bars in Fig. 8, a reliable and definite mode identification using the available diagrams becomes even less likely, certainly when one considers the uncertainties involved in the establishment of the appropriate diagrams. As Watson (1988) points out, there are difficulties such as a worrying large scatter about the $l = 0$ region of interest (for several stars in the $V, B-V$ equivalent diagram) which he, in part, attributes to "the need to take specific models applicable to individual stars, rather than comparing with a single standard model" and other specific effects, such as metallicity. Indeed, we strongly feel that the standard model—as in the case of δ Scuti and 1 Mon, see Watson's solution involving (7400, 3.5, 0.04)—is not applicable for θ Tuc: the effect of using a lower temperature and gravity together with a higher Q should shift the loci of interest upwards in Fig. 8. A model based on (8300, 4, 0.02) as specified in Paper I would rather shift the loci of interest downwards, and outside the area occupied by the measurements. The photometric indices of θ Tuc rather indicate an effective temperature of about 7600 K (not taking into account the possible contamination of the photometric indices by the binary nature) and a slightly lower $\log g$ (Sterken et al. 1997), evoking an upward shift of the loci of interest as is seen in Figs. 18 and 19 of Watson (1988), but with a much larger area for the $l = 0$ and a much smaller area for the $l = 1$ mode (note that in order to achieve consistency between observations and the model in the case of δ Scuti and 1 Mon, Watson also increased by 0.3 the flux derivative $\alpha_T(B)$, a quantity that has a notably steep gradient in the temperature region typically for δ Scuti stars, see his Figs. 18 and 19). This would lead to an assignment $l = 0$ for the principal frequency f_7 (the position with the smallest error bars in Fig. 8) and perhaps allow for a few $l = 2$ modes. We stress, though, that these results are only preliminary guesses, and that it is clear that a definite mode identification with this tool falls beyond the scope of our photometric study since we are handicapped by the scarcity of applicable theoretical results. With support of other mode-identification techniques and with eventual availibility of spectrographic data and at the same time more elaborate theoretical models (allowing, for example, for a tidally-deformed pulsating primary) a definite mode identification will be pursued.

6. Conclusions

We have separated the pulsational and orbital components of the light variation of θ Tuc. The system seems to be an ellipsoidal binary with a $7^{\rm d}.04$ period in which one of the components is a multimode δ Scuti star having a principal frequency that may correspond to an $l = 0$ mode, together with a few other frequencies likely associated with $l = 2$.

Acknowledgements. The author acknowledges a research grant from the Belgian Fund for Scientific Research (FWO) and ESO for the granting of a generous amount of observing time (Period 51). M. Papáro and H.W.W. Spoon are thanked for commenting on the first version of the manuscript. The author is grateful to H.W.W. Spoon for allowing use of the data in advance of publication. E. Poretti is acknowledged for careful proofreading of the manuscript, and the anonymous referee for encouraging remarks.

References

Al-Naimiy, H.M. 1978, ApSS 53, 181
Garrido, R., García-Lobo, E., Rodríguez, E. 1990, A&A 234, 262
Hall, D.S. 1996, in *Light curves of variable stars: a pictorial atlas*, C. Sterken & C. Jaschek (eds.), Cambridge Univ. Press p. 117
Kurtz, D.W. 1988, in *Multimode stellar pulsations*, G. Kovács, L. Szabados, B. Szeidl (eds.), Konkoly Observatory p104
Mantegazza, L., Poretti, E. 1995, AA 294, 190
Morris, S.L. 1985, ApJ 295, 143
Paparó, M., Sterken, C., Spoon, H.W.W., Birch, P.V. 1996 AA 315, 400
Sterken, C., De Mey, K., Gray, R.O. 1997, The Journal of Astronomical Data, submitted
Watson, R.D. 1988, ApSS 140, 255

This article was processed by the author using Springer-Verlag LaTeX A&A style file *L-AA* version 3.